Exploring the potential benefits of Ethanol Direct Injection (EDI) timing and pressure on particulate emission characteristics in a Dual-Fuel Spark Ignition (DFSI) engine

Xiang Li [a, b, *], Dayou Li [a], Jingyin Liu [c, *], Tahmina Ajmal [a], Abdel Aitouche [d, e], Raouf Mobasheri [d, e], Oyuna Rybdylova [f], Yiqiang Pei [b, *], Zhijun Peng [g, *]

[a] School of Computer Science and Technology, University of Bedfordshire, Luton, UK

[b] State Key Laboratory of Engines, Tianjin University, Tianjin, China

[c] School of Chemistry and Chemical Engineering, Nantong University, Nantong, China

[d] Univ. Lille, CNRS, Centrale Lille, UMR 9189 - CRIStAL - Centre de Recherche en Informatique Signal et Automatique de Lille, F-59000 Lille, France

[e] Junia, Smart Systems and Energies, F-59000 Lille, France

[f] Advanced Engineering Centre, School of Architecture, Technology and Engineering, University of Brighton, Brighton, UK

[g] School of Engineering, University of Lincoln, Lincoln, UK

*Corresponding author:

Xiang Li, School of Computer Science and Technology, University of Bedfordshire, Luton, LU1 3JU, UK

Email: xiang.li@beds.ac.uk

Jingyin Liu, School of Chemistry and Chemical Engineering, Nantong, China.

Email: jingyin.liu@ntu.edu.cn

Yiqiang Pei, State Key Laboratory of Engines, Tianjin University, Tianjin, China.

Email: peiyq@tju.edu.cn

Zhijun Peng, School of Engineering, University of Lincoln, Lincoln, LN6 7TS, UK

Email: jpeng@lincoln.ac.uk

Abstract

Nowadays, particulate matter emitted by vehicles severely impacts environmental quality and human health. In this paper, the potential benefits of Ethanol Direct Injection (EDI) timing and pressure on particulate emission characteristics in a Dual-Fuel Spark Ignition (DFSI) engine were initially and systematically explored. The experimental results illustrate that by delaying EDI timing from -340 ºCA to -300 ºCA, there is a significant benefit in both particulate number and mass concentration. Furthermore, the size distribution curve of particulate number changes from bimodal to unimodal, meantime size distribution curves of particulate mass consistently concentrate on the accumulation mode. By increasing EDI pressure from 5.5 MPa to 18 MPa, the droplet size of ethanol spray can be effectively reduced. The benefit of increasing EDI pressure is more apparent in reducing particulate number is than particulate mass. The concentration of number and mass for total particulates have a reduction of 51.15% and 22.64%, respectively. In summary, it was demonstrated that an appropriate EDI timing or high EDI pressure could be a practical and efficient way to reduce particulate emissions in a DFSI engine.

Keywords

Dual-Fuel Spark Ignition (DFSI) engine; Particulate emissions; Ethanol; Injection timing; Injection pressure

1. Introduction

Over the last decade, the impact of environmental pollution has been a global problem. One of the major pollutants is particulate matter emitted by vehicles, which would adversely affect regional air quality, climate change and human health, particularly cardiorespiratory diseases [1]. Currently, some novel vehicle powertrain technologies without Internal Combustion Engine (ICE) have been developed to reduce engine emissions, such as Battery Electric Vehicle (BEV) [2], Fuel Cell Electric Vehicle (FCEV) [3][4], Oxy-Fuel Combustion-Carbon Capture and Storage (OFC-CCS) system [5]. However, the popularisation rate of these technologies is normally subject to cost, cruising range, charging time and relevant supporting facilities [6][7]. Hence, particulate emissions from the ICE of ICE-only vehicle, Hybrid Electric Vehicle (HEV) and Plug-in Hybrid Electric Vehicle (PHEV) have attracted increasing attention from scholars in various fields [8][9].

With the advantages of superior volumetric efficiency, thermal efficiency, power output, and transient response, Gasoline Direct Injection (GDI) engine has become an increasingly prevalent option for ICE and vehicle manufacturers [10][11]. However, compared to Port Fuel Injection (PFI) engine, particulate emissions of GDI engine are usually higher owing to higher spray impingement possibility and shorter air-fuel mixing time [12]. Moreover, the regulations for particulate emissions of GDI-powered vehicles have become more stringent in recent years. For example, in 2014 and 2017, Euro 6b and Euro 6c standards limit the particulate number of GDI-powered vehicles to 6×10^{12}/km and 6×10^{11}/km, respectively.

In order to reduce particulate emissions and keep the engine power performance, Dual-Fuel Spark Ignition (DFSI) engine has been developed with the advantages of multiple fuel injection modes and fuel properties [13]. Due to higher heating value and lower vaporisation latent heat, gasoline can be used to contribute a better transient response, especially during engine cold start. As renewable fuels with low carbon and high oxygen content, alcohol fuel can be utilised to reduce engine particulate emissions and improve anti-knock performance by the advantage of higher octane.

The important research findings relevant to Dual-Fuel Spark Ignition (DFSI) engines are summarised in Table 1. Daniel et al. [14] found that with the advantages of fuel injection flexibility, Dual-Fuel Spark Ignition (DFSI) is very beneficial to optimise engine gaseous and particulate emissions with changes in engine operating conditions. Kim et al. [15] demonstrated that both reduction of particulate emissions and knock frequency could be achieved when ethanol port injection is added. Liu et al. [16][17] compared different alcohol–gasoline and gasoline–alcohol injection modes from a DFSI combustion engine. It was found that for selected engine operating conditions, there is an optimal mass fraction for alcohol injection to optimise particulate matter emissions and simultaneously keep fuel economy and power output. Catapano et al. [18] observed particulate formation and emissions in an optical small DFSI engine fuelled with Compressed Natural Gas (CNG) and gasoline. It was demonstrated that there is a benefit in reducing particulate emissions owing to the gaseous properties of CNG. Kang et al. [19] systematically compared the effects of different injection modes on combustion and knock suppression characteristics. Yu et al. [20][21] conducted experimental studies about combustion and emissions in an SI engine, with ethanol/gasoline and hydrous ethanol/gasoline dual-fuel injection modes. The studies concluded that the synergistic effects of utilising ethanol injection and Exhaust Gas Recirculation (EGR) could effectively reduce gas and particulate emissions. Furthermore, particulate size can be reduced by increasing the water ratio in hydrous ethanol. Zhuang et al. [22][23] investigated the effects of different ethanol Direct Injection (DI) timings on air-fuel mixture formation, combustion process, knock mitigation, Nitrogen Oxide (NO) and Hydrocarbon (HC) emissions from a DFSI engine. It was indicated that ethanol DI timing strongly influences the air-fuel mixture process and quality. Moreover, with the advance of ethanol

DI timing, the emissions are generally decreased.

Table 1. Important research findings concerning DFSI engines

Publication Year	Key Advances	Fuel	Main Authors
2013	Particulate emissions were investigated for ethanol injection under both dual-fuel injection and DI strategies.	Ethanol; Gasoline	Daniel et al. [14]
2014	Effects of ethanol injection timing on knock mitigation, lean-burn, NO and HC emissions were investigated from an SI engine with PFI-gasoline and DI-ethanol.	Ethanol; Gasoline	Zhuang et al. [22]
2015	Particulate emissions were investigated in an SI engine with PFI-ethanol and DI-gasoline with varying engine compression ratios and ethanol injection timings.	Ethanol; Gasoline	Kim et al. [15]
2015	The alcohol–gasoline and gasoline–alcohol DFSI combustion was compared for particulate reduction and fuel economy with varying alcohol mass fractions.	Methanol; Ethanol; Gasoline	Liu et al. [16][17]
2017	Particulate emissions were investigated in an optical small DFSI engine with DI-CNG and PFI-gasoline.	CNG; Gasoline	Catapano et al. [18]
2019	Effects of fuel injection modes on knock suppression were compared and studied under different injection modes on a single-cylinder SI engine.	Ethanol; Gasoline	Kang et al. [19]
2020	Effects of ethanol injection strategies on air-fuel mixture formation and combustion process were investigated from an SI engine with PFI-gasoline and DI-ethanol.	Ethanol; Gasoline	Zhuang et al. [23]
2021	The combustion and emissions were investigated with varying access air ratios, ethanol direct injection ratios and exhaust recirculation ratios from an SI engine with PFI-gasoline and DI-ethanol.	Ethanol; Gasoline	Yu et al. [20]
2021	Effects of different water ratios in hydrous ethanol on combustion and emissions were investigated from an SI engine with PFI-gasoline and DI-hydrous ethanol.	Ethanol; Gasoline	Yu et al. [21]

As mentioned above, previous studies on the DFSI engine have proposed and investigated some effective solutions to reduce engine emissions. However, regarding the fuel injection strategies of DFSI engines, research findings mainly focused on the influence of fuel injection ratios and timings on gaseous emissions. Besides, the effects of ethanol injection ratio on particulate emissions are another existing hot topic. However, almost no systematic study on the effects of Ethanol Direct Injection (EDI) timing and pressure on particulate emissions in a DFSI engine was reported.

Hence, the study presented in this paper concentrates on exploring the benefits of EDI timing and pressure on particulate emission characteristics from a DFSI engine. The findings of this study would help not only fill the gap of exploring EDI strategy on the reduction of particulate, but also provides a fresh and practical way towards controlling the particulate problem of different kinds of vehicles.

2. Experimental methodology

2.1. Experimental testbed and procedure

The experimental study was performed on a dual-injection DFSI engine with the specifications shown in Table 2. It is an advanced four-cylinder turbocharged engine with a displacement of 2.0-litre and a compression ratio of 9.6. The fuel properties of gasoline and ethanol used in this study are both presented in Table 3 [24]. Furthermore, as shown in Fig. 1, gasoline and ethanol are injected via PFI injectors and DI injectors, respectively.

Table 2. Engine specifications

Items	Content
Engine type	4-cylinder, 4-stroke
Bore × Stroke (mm)	82.5 × 92
Displacement (L)	2.0
Injection mode	Dual-injection
Intake mode	Turbocharged
Compression ratio	9.6:1
Rated speed (rpm)	5500
Rated power (kW)	160
Maximum Torque (N·m)	320

Table 3. Fuel properties [24]

Fuel type	Ethanol	Gasoline
Chemical formula	C_2H_5OH	C5-C12
Relative molecular mass	46	95-120
Gravimetric oxygen content (%)	34.78	< 1
Research octane number	107	95

Density (20 °C) (kg/L)	0.789	0.73
Dynamic viscosity (20 °C) (mPa·s)	1.2	0.52
Kinematic viscosity (20 °C) (mm^2/s)	1.52	0.71
Surface tension (20 °C) (N/m)	21.97	22
Boiling range (°C)	78	30-200
Low heating value (kJ/kg)	26900	44300
Latent heat of vaporisation (kJ/kg)	840	370
Laminar flame speed (20 °C) (m/s)	0.5	0.33
Stoichiometric air-fuel ratio	8.95	14.7

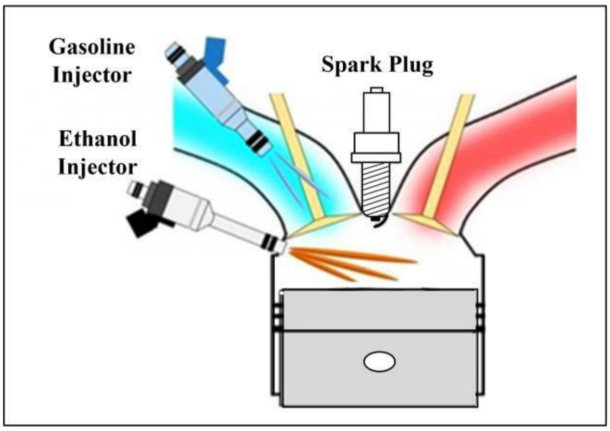

Fig. 1. Schematic view of GPI plus EDI dual-injection system

Fig. 2 shows the schematic view of engine testbed. By using a programmable Electronic Control Unit (ECU) and calibration software (INCA), an electrical dynamometer can measure and control engine speed, torque and power output in real-time. Combustion characteristics can be calculated by the transient signals of in-cylinder pressure, which were recorded and analysed via a combustion measurement platform, including four high-precision spark-plug pressure sensors (AVL-GH13Z), an encoder (Kistler-2614CK1), charge amplifiers (Kistler-5018A) and a combustion analyser (AVL-641). In addition, the emission of particulates ranging from 5 nm to 1000 nm was measured by a fast particulate analyser (Cambustion-DMS 500) connected to a sampling point in front of the engine's three-way catalytic converter. In this study, the engine operated at the speed of 2000 revolutions per minute (rpm) and a typical low load of 2 bar Brake Mean Effective Pressure (BMEP). In order to make the research process more efficient, the fuel injection mass ratio of PFI to DI was fixed at 1:1, representing 50% gasoline-PFI plus 50% ethanol-DI.

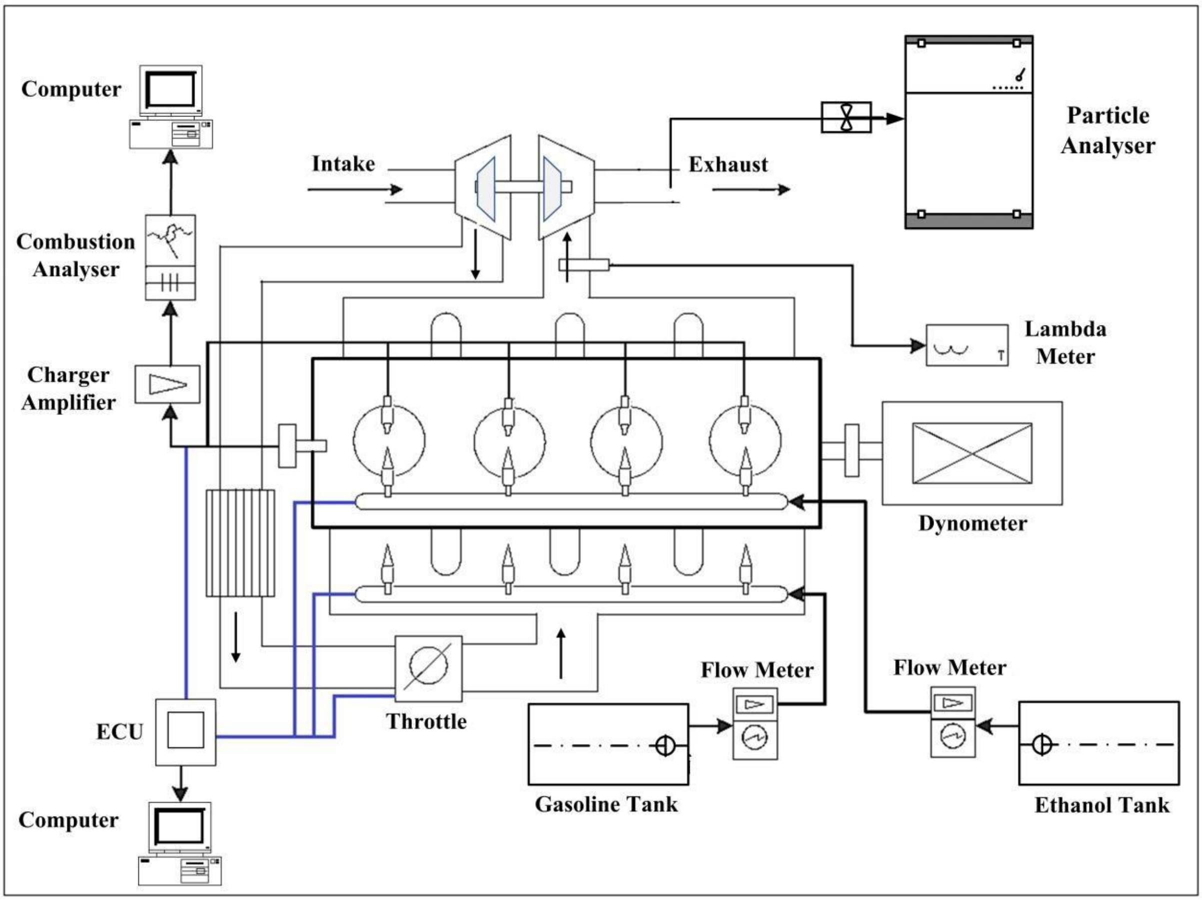

Fig. 2. Schematic view of engine testbed

In order to assure the accuracy of experimental results, Maximum Brake Torque (MBT) spark timings were applied to all the engine operating conditions. The lambda, intercooler outlet temperature and coolant were maintained at 1 ± 0.01, 298 ± 2 K and 360 ± 2 K, respectively. The combustion characteristics and particulate emissions data for each engine operating condition should be recorded after the engine stabilises for two minutes. Furthermore, to minimise the impacts of cycle-to-cycle variations, cylinder pressure result was averaged based on two hundred consecutive engine cycles. Meanwhile, the result of particulate emissions was obtained from the average of repeated measurements three times. Table 4 presents the uncertainties of some key parameters calculated by Holman's root mean square method [25].

Table 4. Uncertainties of measured parameters

Measured Parameters	Uncertainty (%)
Engine speed	± 0.1
BMEP	± 0.1
BSFC	± 0.2
Pressure	± 0.1
Crank angle	± 0.1
Lambda	± 0.3
Coolant temperature	± 0.4
Intercooler output temperature	± 0.4
Particulate number	± 1.7

In order to make this research more comprehensive, the effects of EDI pressure on the droplet diameter of ethanol spray from the engine's DI injector were studied via microscopic spray characteristics investigation. Fig. 3 shows the Phase Doppler Particles Analyser (PDPA) system for this investigation. With the advantage of an argon-ion laser, a 180 MHz high-frequency signal processor and some other accessories, the PDPA system can provide accurate measurement results of droplet diameter with a high resolution of 0.1 μm and a range from 0 to 236 μm. In order to match with engine experiments, EDI pressure was set to be 5.5 MPa, 10 MPa, 14 MPa and 18 MPa in this test. Furthermore, ethanol was injected into an ambient condition, which is 293 ± 0.5 K and 0.1 MPa. An air extractor was utilised to help ensure the safety of experimental site.

Besides, as shown in Fig. 4, according to the Society of Automotive Engineers (SAE) J2715 standard [26], measurement points are selected at 50 mm downstream from the axial direction of the nozzle. For minimising the interference of suspended fuel droplets of the latest injection, the ethanol injection pulse and injection width were set to 0.1 Hz and 1.2 ms, respectively. To ensure measurement accuracy, 20000 validated sample droplets were collected for each experimental condition, and the collection should be repeated three times.

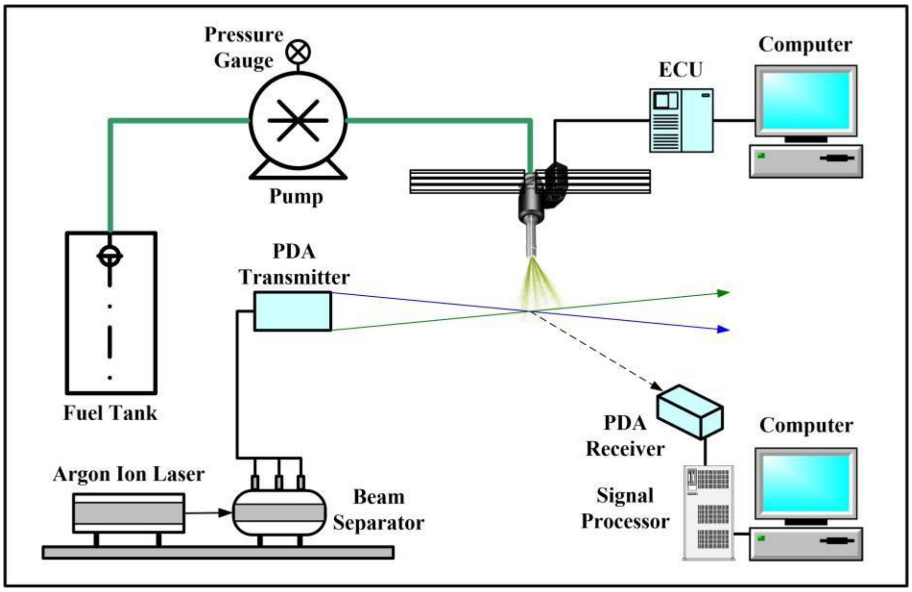

Fig. 3. Schematic view of PDPA system

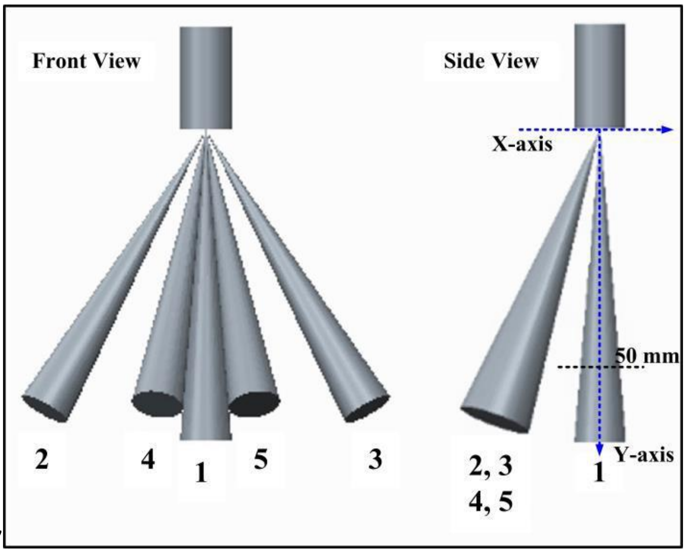

Fig. 4. Measurement points of PDPA test

2.2. Key parameters in this study

In this study, some key parameters are introduced and defined to help better under the characteristics of combustion and particulate emissions. t_I and P_I denote EDI timing and EDI pressure, respectively. θ_F denotes ignition delay, representing Crank Angle (CA) interval between spark timing and φ_{CA10} (where 10% of cumulative heat has released). θ_C denotes combustion duration, representing CA interval between φ_{CA10} and φ_{CA90} (where 90% of cumulative heat has released). φ_{CA50} denotes the CA where 50% of cumulative heat has released. R_M and T_M denote maximum heat release rate and maximum in-cylinder temperature, respectively. η_B denotes engine brake thermal efficiency, as shown in Equation (1).

$$\eta_B = \frac{p_B}{M_G \times H_G + M_E \times H_E} \times 100\% \tag{1}$$

Here, p_B is engine brake power. M_G and M_E are the mass flow rate of gasoline and ethanol, respectively. M_G and M_E are the mass flow rate of gasoline and ethanol, respectively. H_G and H_E are the low heating value of gasoline and ethanol, respectively.

Regarding the parameters of particulate emissions, D_P, N_P and M_P denote particulate diameter, particulate number and particulate mass, respectively. For each particulate, the calculation of converting D_P to M_P is shown in Equation (2) [27][28].

$$M_P(\mu g) = 1.72 \times 10^{-15} \times D_P^{2.65}(nm) \tag{2}$$

Besides, in the PDPA test, D_d denotes diameter of droplet; D_{SMD} denotes Sauter mean diameter of droplets; D_{sub} denotes the difference of D_{SMD} between P_I = 5 MPa and other P_I (10 MPa, 14 MPa and 18 MPa) conditions.

3. Results and discussion

3.1. Optimising engine particulate emission characteristics by changing EDI timing

In the section, the characteristics of particulate emission are investigated by changing t_I from -340 ºCA to -280 ºCA. Meantime, P_I is fixed at base value, which is 5.5 MPa.

Fig. 5 shows the effects of t_I on θ_F, θ_C, φ_{CA50} and η_B. On the whole, combustion phasing characterised by θ_F, θ_C and φ_{CA50} is not significantly affected by t_I, but some key features can also be observed.

With the delay of t_I from -340 ºCA to -280 ºCA, θ_F slightly increases from 27.06 degrees to 27.37 degrees, meantime θ_C has a reduction of 0.68 degrees. Besides, the variation of φ_{CA50} is generally stable with the delay of t_I. As a result, η_B shows a slight improvement of 0.21 percent. This can be attributed to a combined effect of three factors. First, as the earliest injection condition (t_I = -340 ºCA) is very near to Top Dead Centre (TDC), it is easy to cause fuel impingement on the piston crown, slowing down the rate of fuel vaporisation. Hence, delaying t_I to -280 ºCA would help reduce the possibility of fuel impingement, which is beneficial to promote air-fuel mixture. Second, under t_I = -280 ºCA, θ_C becomes shorter which helps reduce the heat transfer to combustion chamber walls. Third, by delaying t_I, the homogeneity of air-fuel mixture would be reduced owing to a shorter mixing time. It would lead to a negative impact on η_B, but it cannot offset the first two benefits.

Fig. 6 and Fig. 7 show the effects of t_I on cylinder pressure and heat release rate, respectively. It is demonstrated that there is no obvious change in the curves of cylinder pressure and heat release rate by changing t_I. The main feature is that with the delay of t_I from -340 ºCA to -280 ºCA, there is a slight rise in the peak of the curve. Fig. 8 presents the effects of t_I on R_M and T_M. It can be seen that with the delay of t_I, R_M shows a general gradual increase of 0.56 J/CA. In the meantime, T_M is a bit lower when t_I is -320 ºCA and -300 ºCA, but it keeps around 2575 K on the whole, which indicates that the probability of particulate oxidation is not greatly affected by the variation of T_M under different conditions of t_I.

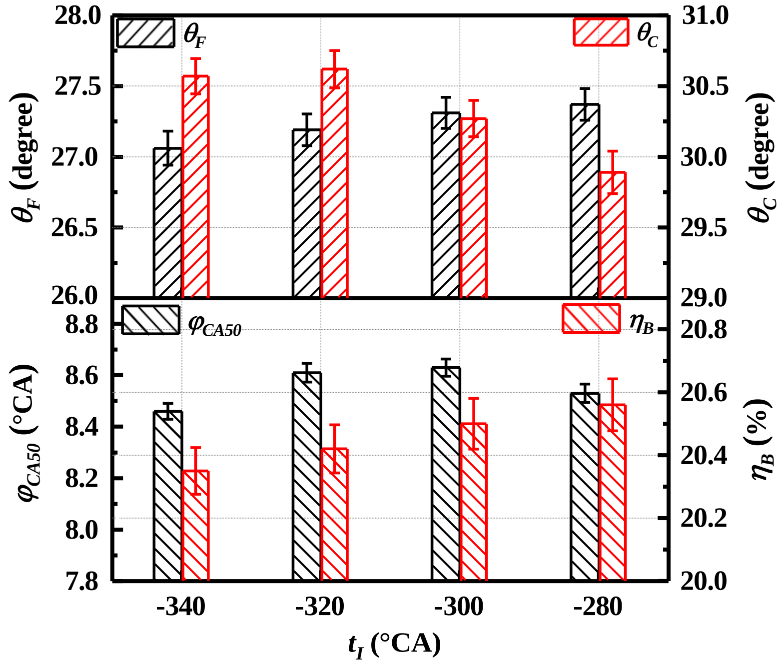

Fig. 5. Effects of t_I on θ_F, θ_C, φ_{CA50} and η_B

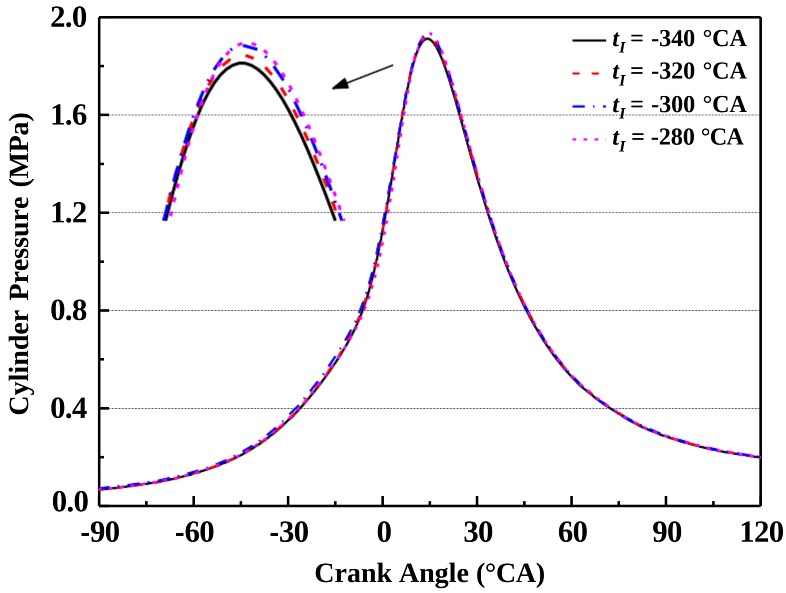

Fig. 6. Effects of t_I on cylinder pressure

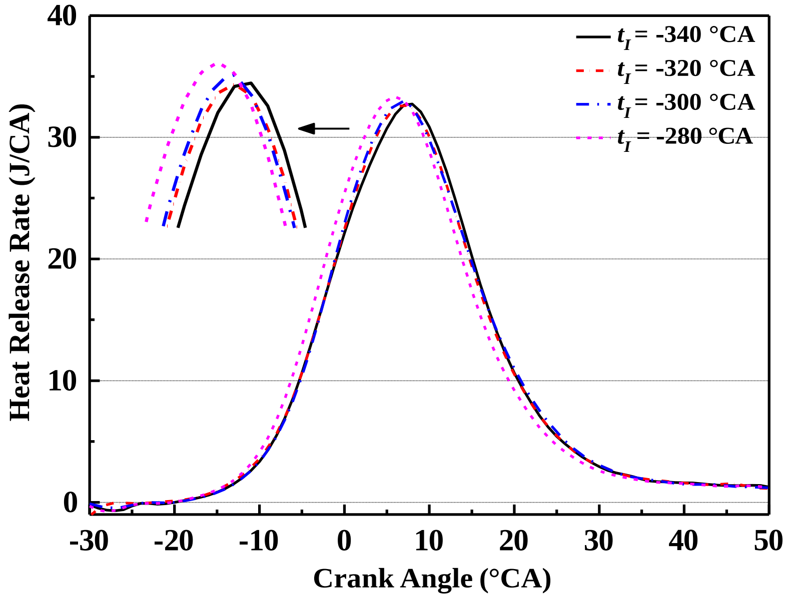

Fig. 7. Effects of t_I on heat release rate

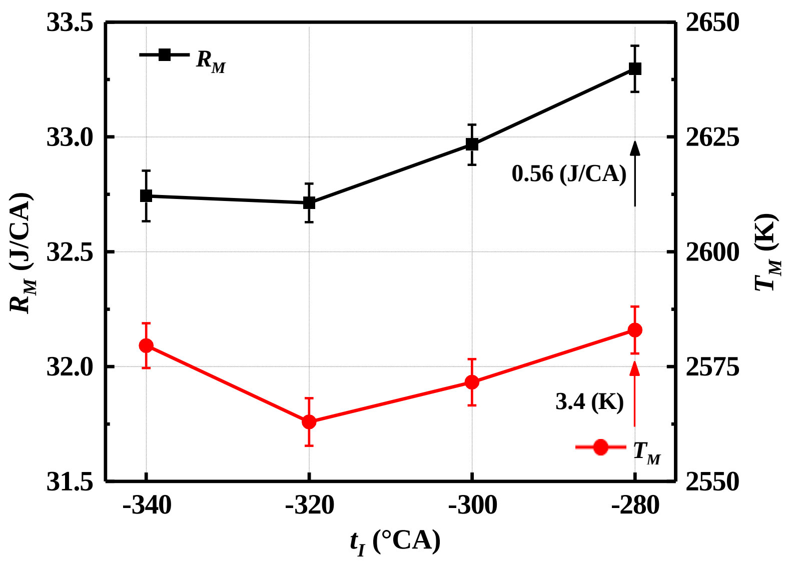

Fig. 8. Effects of t_I on R_M and T_M

Fig. 9 shows the effects of t_I on N_P size distribution. It can be seen that the N_P size distribution is quite sensitive to t_I. With t_I from -340 ºCA to -320 ºCA, the peak of curve for nucleation mode decreases from 1.27×10^6 to 8.36×10^5, whilst the peak of accumulation mode decreases from 1.48×10^6 to 6.45×10^5. By delaying t_I to -300 ºCA, the curve changes from bimodal to unimodal. However, it would increase again and change to be bimodal again with the further delay of t_I to -280 ºCA. This is mainly because when t_I is -340 ºCA, the piston has just passed through the TDC. The spray impingement possibilities will be significantly increased, as the fuel injector is relatively close to piston crown. When t_I is -280 ºCA, heterogeneous mixture will also be enhanced by less time between t_I and spark timing compared to that of t_I = -300 ºCA. Besides, Hydrogen-Abstraction-Acetylene-Addition (HACA) growth rates would be increased with a higher T_M when t_I is -340 ºCA and -280 ºCA [29][30]. Thus, the quality of air-fuel mixture has deteriorated, leading to higher emissions of N_P.

Fig. 10 shows the effects of t_I on M_P size distribution. Regardless of t_I, M_P size distribution almost concentrates on the accumulation mode, meantime M_P of nucleation mode is very low. Besides, the highest M_P curve can be seen under the condition of t_I = -340 ºCA due to the largest N_P of accumulation mode under this condition.

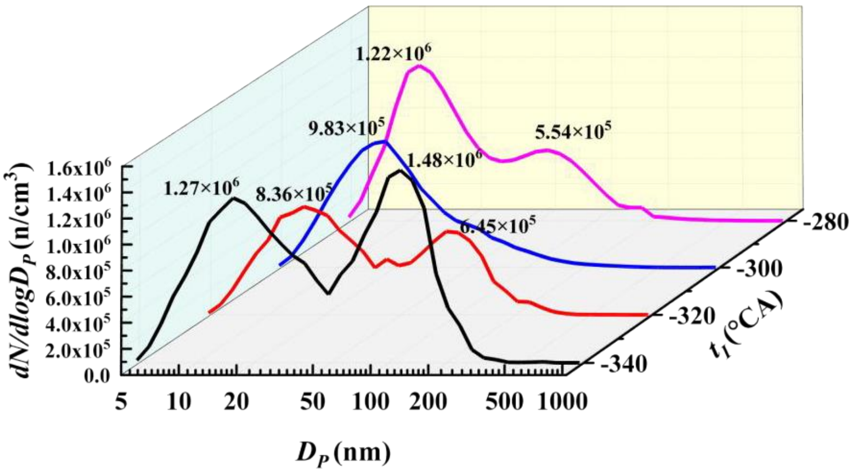

Fig. 9. Effects of t_I on N_P size distribution

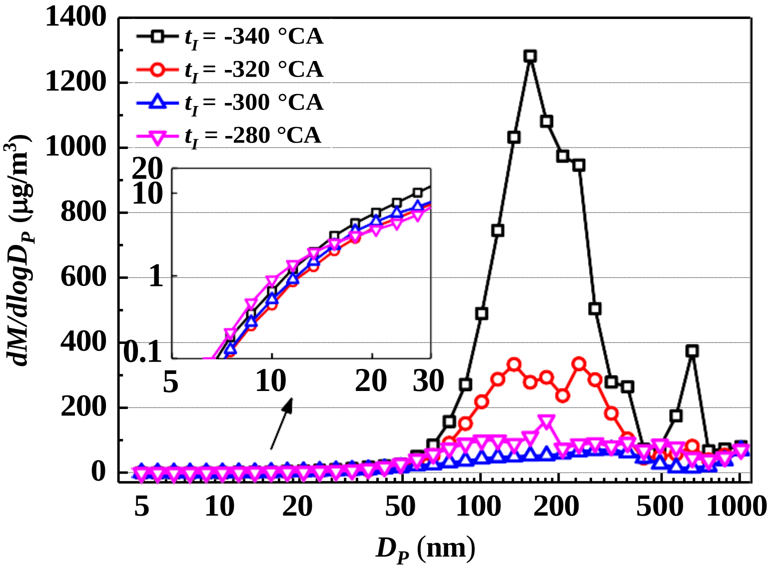

Fig. 10. Effects of t_I on M_P size distribution

In order to better understand the effects of t_I on particulate emissions at a macroscopic level, Fig. 11 and Fig. 12 presents the N_P and M_P concentrations with varying t_I, respectively.

It can be seen that both N_P and M_P concentrations are very sensitive to changing t_I. On the whole, an appropriate t_I is very helpful to decrease particulate emissions. By delaying t_I from -340 ºCA to -300 ºCA, there is a significant reduction of 54.65 % and 89.15% in N_P concentration and M_P concentration of total particulates, respectively. But the immediate cause of reduction for N_P concentration is not very similar to that of M_P. Under t_I = -300 ºCA, although N_P of nucleation mode is a bit higher than that of t_I = -320 ºCA owing to the less air-fuel mixture time, N_P concentration of total particulates is still lower under t_I = -300 ºCA by the significant reduction in accumulation particulates. Regarding the M_P concentration, M_P of nucleation mode can be neglected, so M_P concentration of total particulates is closely related to accumulation mode.

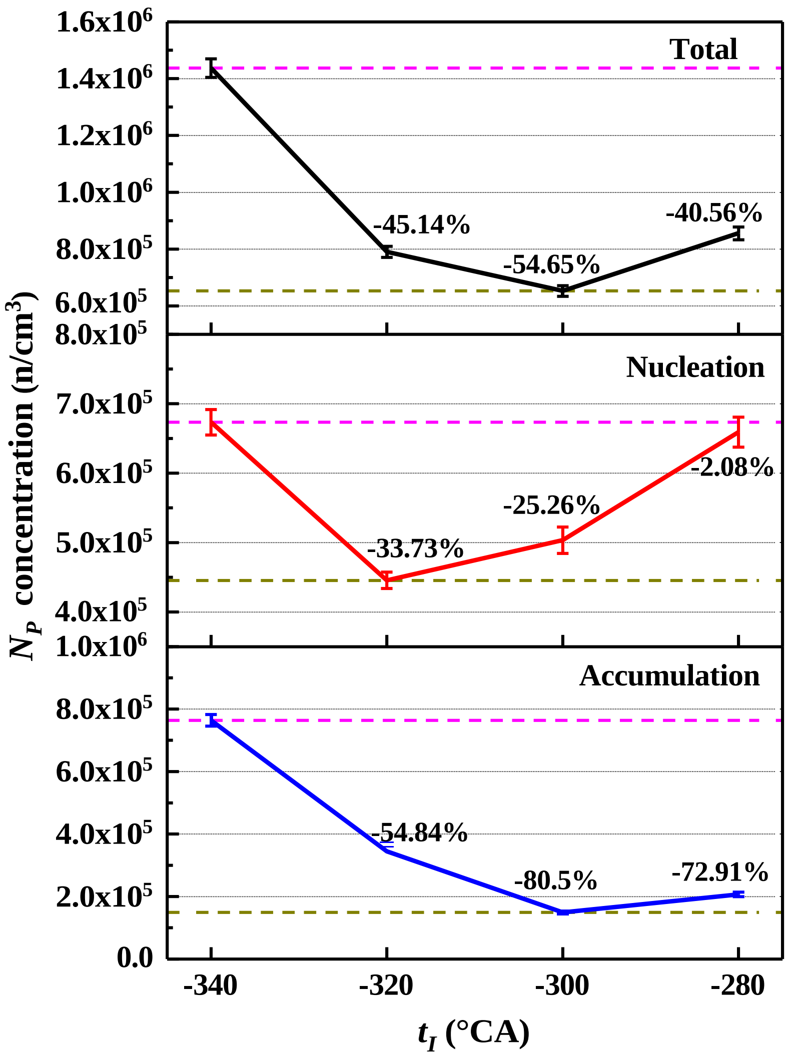

Fig. 11. Effects of t_I on N_P concentration for nucleation, accumulation and total particulates

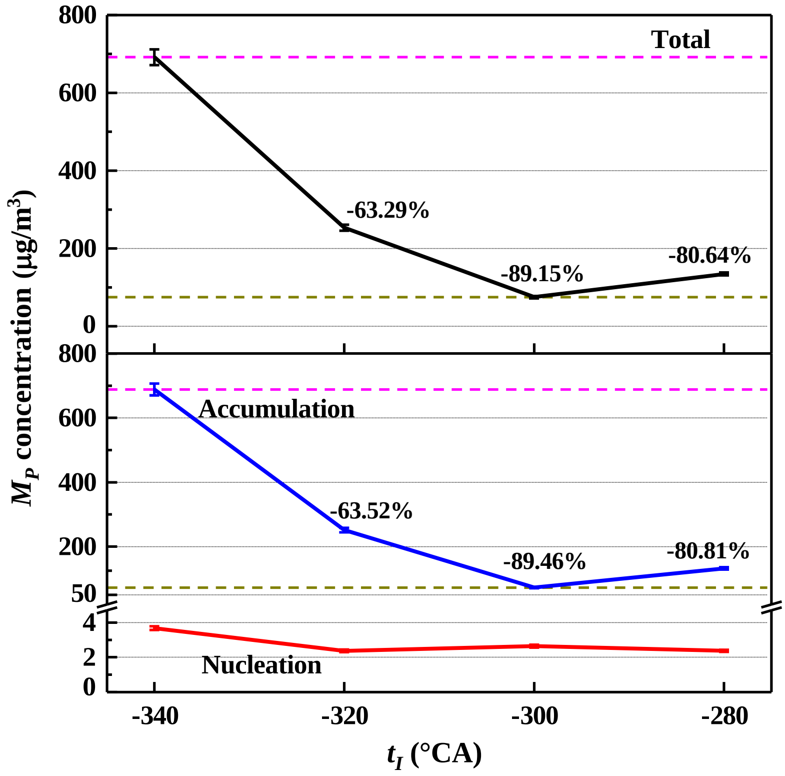

Fig. 12. Effects of t_I on M_P concentration for nucleation, accumulation and total particulates

3.2. Optimising engine particulate emission characteristics by EDI pressure

This section mainly focuses on the experimental results by changing P_I from 5.5 MPa to 18 MPa, which covers the P_I common range of most commercial GDI and DFSI engines. Moreover, t_I is fixed at -300 ºCA in the meantime.

Fig. 13 presents the effects of P_I on p_d of D_d at (0, 50). It can be seen that with the increase of P_I from 5.5 MPa to 18 MPa, a steady decline can be found in the p_d of large droplets which D_d is more than 20 μm. Furthermore, the concentration of D_d moves to smaller size droplets. The position and p_d of curve's peak respectively change to 6 μm and 14.8% under P_I = 18 MPa, while the corresponding values are respectively 10 μm and 11.55% under P_I = 5.5 MPa.

Regarding the whole view of droplet size at 50 mm of jet downstream, Fig. 14 shows the effects of P_I on both D_{SMD} and D_{Sub} for different locations. It was found that increasing P_I can effectively decrease D_{SMD} regardless of the locations, which would promote the progress of secondary atomisation, evaporation and air-fuel mixing. Besides, the comparison of D_{sub} of different P_I denotes that a reduction of around 1.7 μm can be observed for every 4 MPa increase of P_I. Another interesting observation is that D_{SMD} of (-12, 50) and (12, 50) is larger than locations. This explanation can be that the bulk of the spray breaks into filaments and droplets during the primary atomisation, increasing the collision probability between droplets inside the spray boundary. In the meantime, the breakup rate is increased by the shearing force outside the spray boundary, reducing the D_{SMD} of (-16, 50) and (16, 50). As a result, the curves present a general distribution of bimodal under all conditions of P_I.

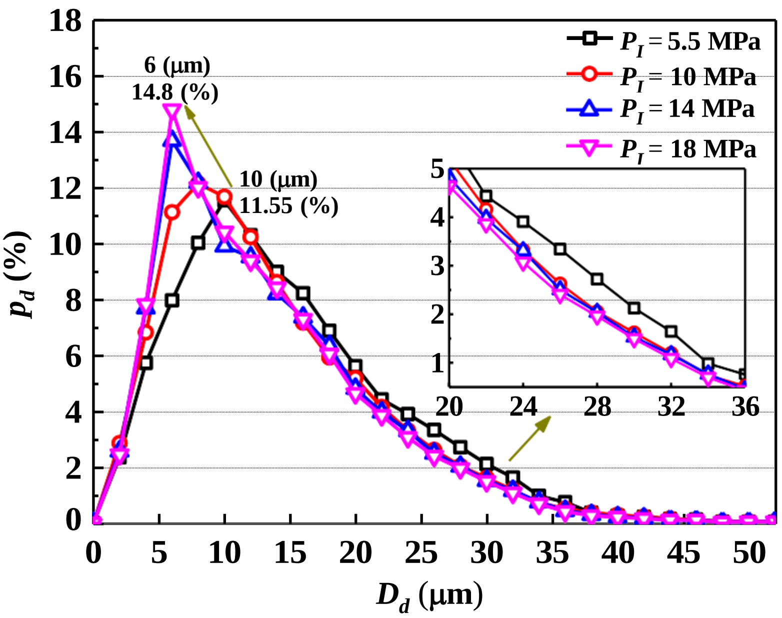

Fig. 13. Effects of P_I on p_d of D_d at (0, 50)

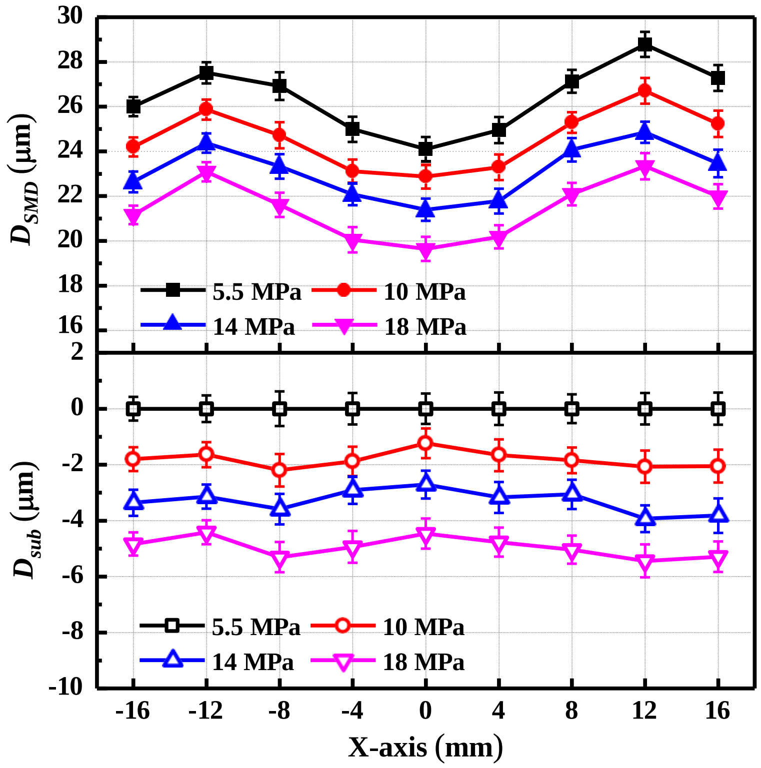

Fig. 14. Effects of P_I on D_{SMD} and D_{Sub} at 50 mm of jet downstream

Fig. 15 presents the effects of P_I on θ_F, θ_C, φ_{CA50} and η_B. It can be seen that increasing P_I could reduce the combustion duration, even though the effect is not apparent. With the increase of P_I from 5.5 MPa to 18 MPa, θ_F and θ_C each reduces 0.72 degrees and 0.47 degrees, meanwhile φ_{CA50} slightly advances from 8.63 ºCA to 8.51 ºCA. This is because the air-fuel mixture quality is improved with the reduction of D_{SMD} owing to higher P_I. A shorter combustion duration would mitigate the waste heat between high-temperature gases and in-cylinder wall, leading to a benefit of 0.13 percent in η_B. Fig. 16 and Fig. 17 present the variations of cylinder pressure and heat release rate with varying P_I. On the whole, both of them are not significantly affected by P_I. The main characteristic is that a slight advance and improvement can be observed for the curve' peak by increasing P_I. Fig. 18 further shows that there is a gradual increase of R_M and T_M with the increase of P_I, which could help promote fuel burn rate, leading to a benefit in η_B.

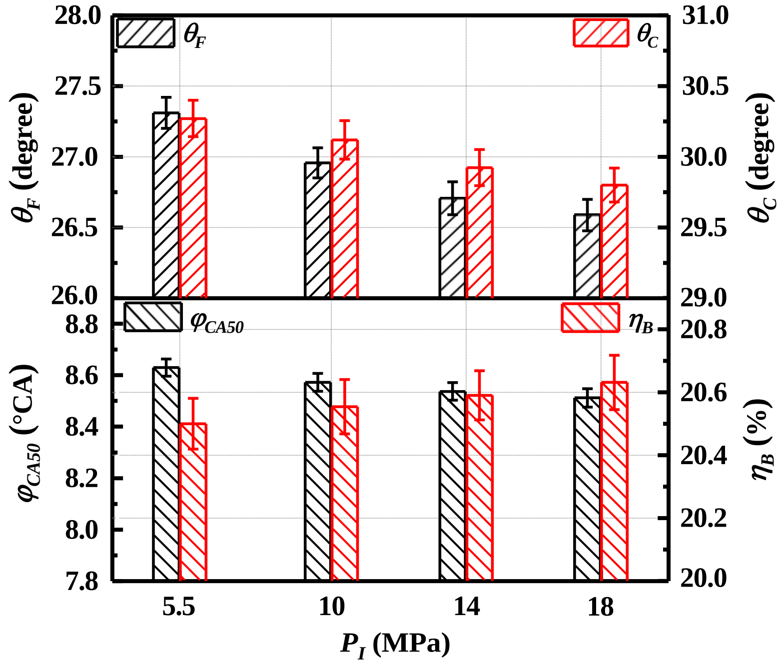

Fig. 15. Effects of P_I on θ_F, θ_C, φ_{CA50} and η_B

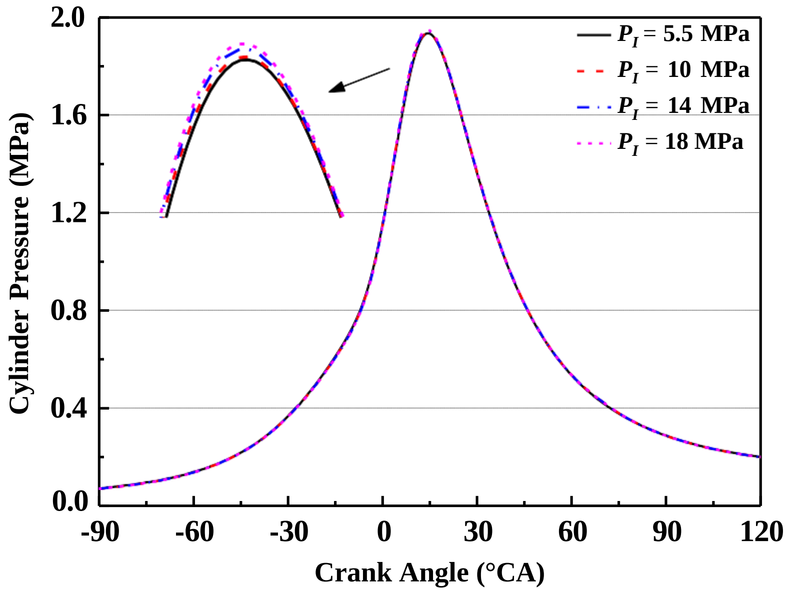

Fig. 16. Effects of P_I on cylinder pressure

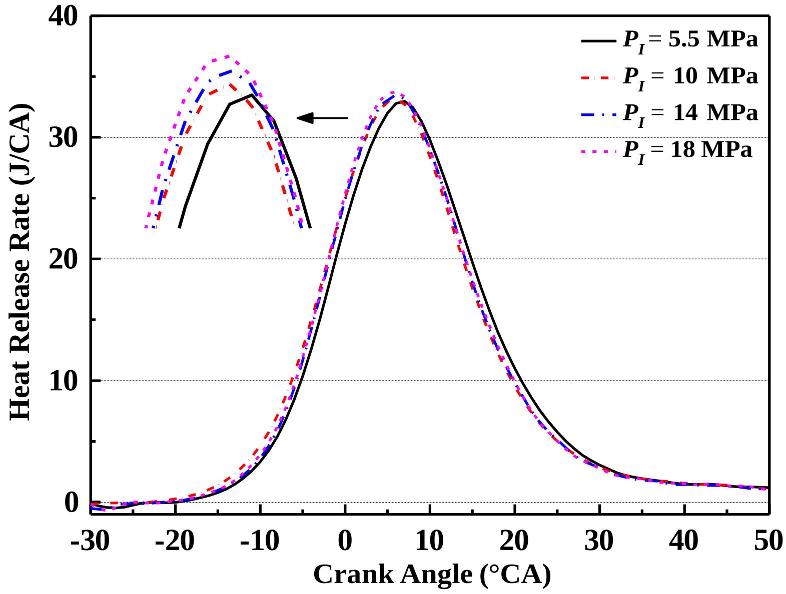

Fig. 17. Effects of P_I on heat release rate

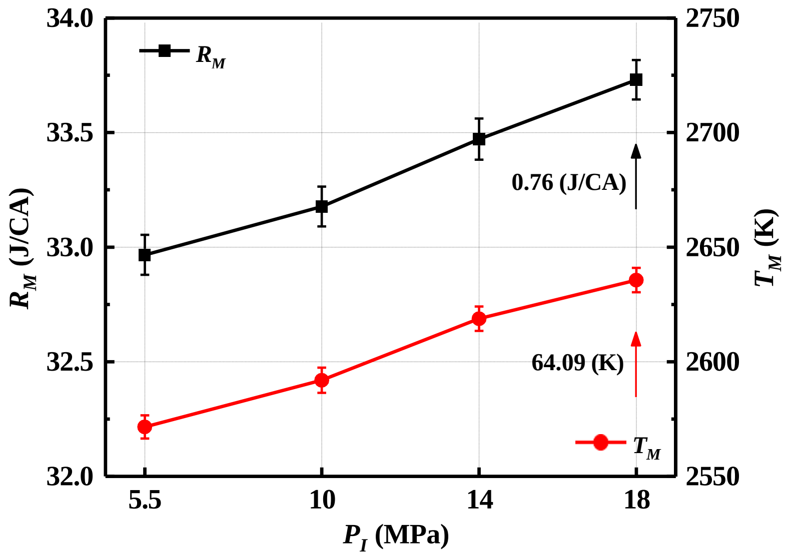

Fig. 18. Effects of P_I on R_M and T_M

Fig. 19 and Fig. 20 show the effects of P_I on size distribution of N_P and M_P, respectively. It can be observed that every N_P curve presents an approximate unimodal distribution with a peak located around 17 nm nucleation mode. Furthermore, by increasing P_I from 5.5 MPa to 18 MPa, the peak of N_P curve gradually reduces from 9.83×10^5 to 4.66×10^5. Regarding the trend of M_P, it demonstrates that increasing P_I has a positive effect on M_P reduction, but the benefit is not very obvious. The curve shape of M_P size distribution remains stable, and the curve peak concentrates around 300 nm D_P. Besides, because a large nucleation particulate is much heavier than nucleation particulates, an increment can be seen for D_P more than 600 nm in the M_P curves. But due to the very small N_P, the absolute value of M_P is still very low, which is less than 70 at 1000 nm.

Fig. 21 and Fig. 22 can visually explain the effects of P_I on N_P and M_P in a macroscopic view. With the increase of P_I from 5.5 MPa to 18 MPa, the concentration of N_P and M_P for total particulates decrease by 51.15% and 22.64%, respectively. The reduction of M_P is far less than that of N_P. Moreover, M_P concentration of total particulates is closely related to that of accumulation mode, which presents a gradual decline trend with increased P_I. This is because regardless of P_I, EDI mode would have the appearance of spray impingement, which causes the heterogeneous mixture around piston crown region. Although higher P_I is helpful to air-fuel mixture quality, the heterogeneous mixture by spray impingement and pool fires cannot be entirely avoided, which is a dominant source of accumulation mode particulates. Besides, Fig. 18 has demonstrated that higher in-cylinder temperature can be seen with increased P_I, which would further gain the advantage of promoting particulate oxidation by ethanol as an oxygenated fuel, providing a benefit in the reduction of N_P and M_P.

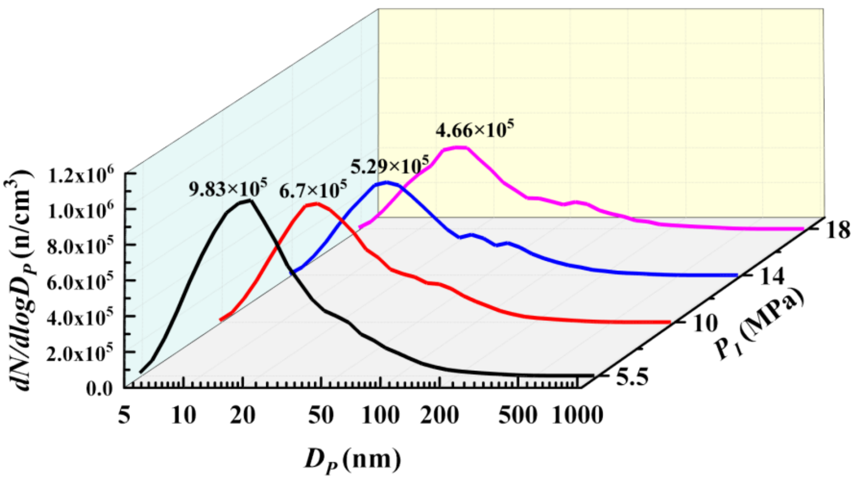

Fig. 19. Effects of P_I on N_P size distribution

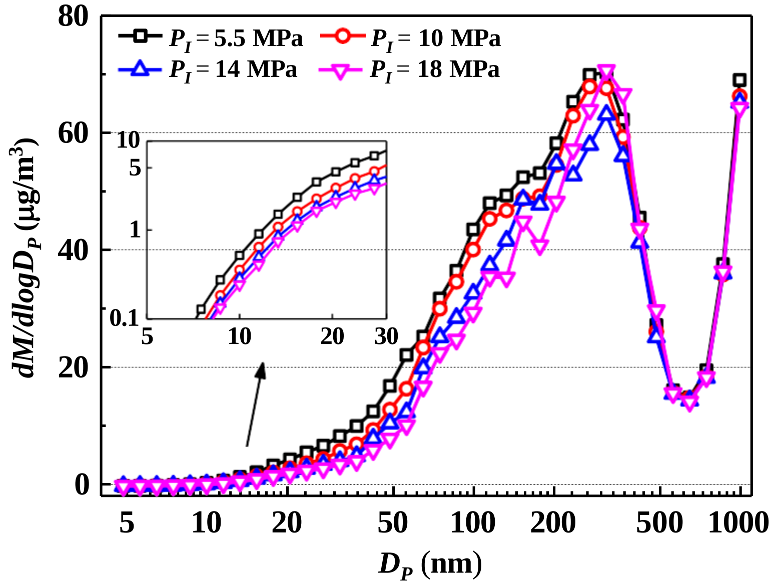

Fig. 20. Effects of P_I on M_P size distribution

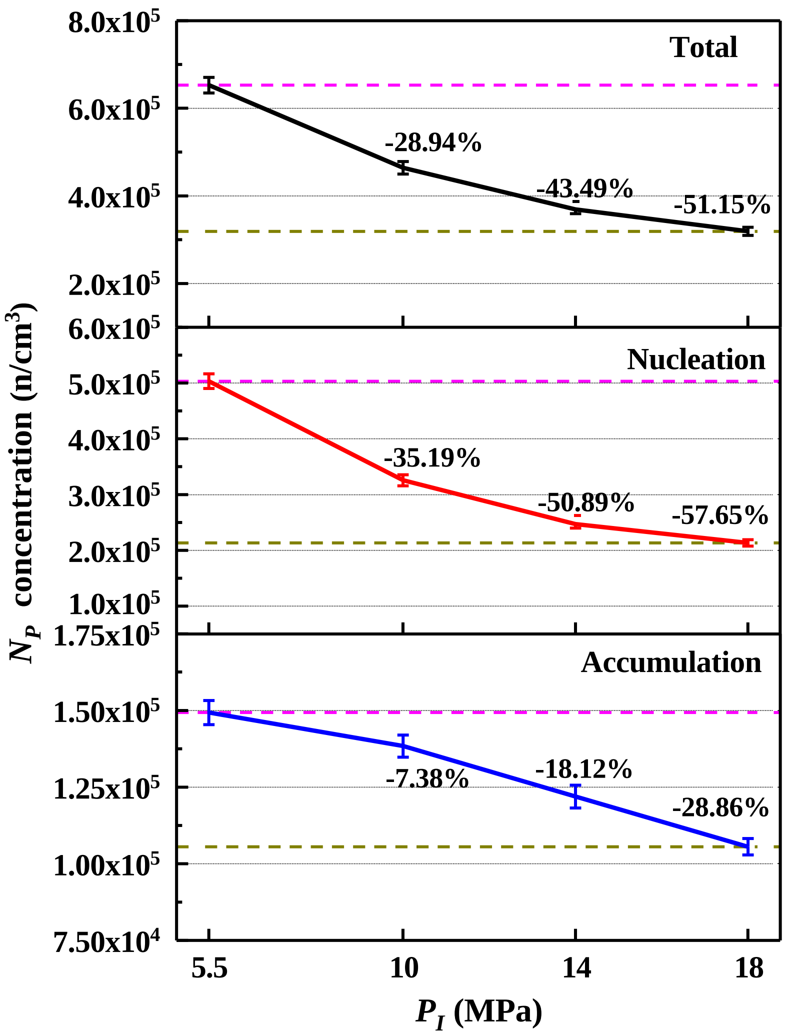

Fig. 21. Effects of P_I on N_P concentration for nucleation, accumulation and total particulates

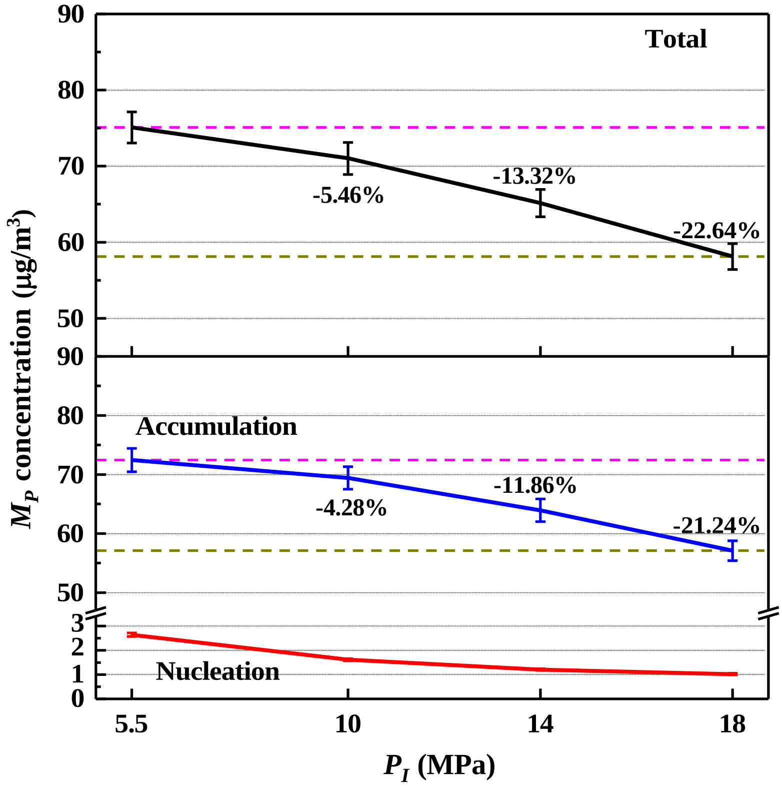

Fig. 22. Effects of P_I on M_P concentration for nucleation, accumulation and total particulates

4. Conclusions

In order to develop more environmentally friendly vehicles, particulate emissions from ICE have been a serious problem to solve. The importance of this study is that the potential benefits of EDI timing and pressure on particulate emissions are systematically explored in a DFSI engine under PFI-gasoline and DI-ethanol mode. The findings can offer some original and fresh insights into the implementation of ethanol combined with the injection strategy of controlling particulate emissions regarding the DFSI engine. The main results of this study can be drawn as follows.

(1) With the delay of t_I from -340 ºCA to -280 ºCA, θ_C has a reduction of 0.68 degrees. The variations of θ_F and φ_{CA50} are generally stable. In the meantime, a slight improvement of 0.21 percent in η_B can be achieved.

(2) It is a highly effective way to optimise engine particulate emission characteristics by changing t_I. By delaying t_I from -340 ºCA to -300 ºCA, there is a significant reduction of 54.65 %

and 89.15% in N_P concentration and M_P concentration of total particulates, respectively. Furthermore, the curve of N_P size distribution changes from bimodal to unimodal. Under all conditions, M_P size distribution almost concentrates on the accumulation mode.

(3) Increasing P_I would promote the progress of secondary atomisation, evaporation and air-fuel mixing for the ethanol spray. By increasing P_I from 5.5 MPa to 18 MPa, the position and p_d of curve's peak respectively change to 6 μm and 14.8% from 10 μm and 11.55%. D_{SMD} can be effectively reduced.

(4) By increasing P_I from 5.5 MPa to 18 MPa, the gradual increase of R_M and T_M could help promote fuel burn rate. θ_F and θ_C each reduce 0.72 degrees and 0.47 degrees, meanwhile φ_{CA50} slightly advances from 8.63 ºCA to 8.51 ºCA, leading to a benefit of 0.13 percent in η_B.

(5) Regardless of P_I, N_P curve presents an approximate unimodal distribution with a peak located around 17 nm nucleation mode. With the increase of P_I to 18 MPa, it is more apparent in the reduction of N_P is than that of M_P. The concentration of N_P and M_P for total particulates decrease by 51.15% and 22.64%, respectively.

CRediT authorship contribution statement

Xiang Li: Conceptualization, Methodology, Formal analysis, Investigation, Data curation, Visualization, Writing - original draft. **Dayou Li:** Formal analysis. **Jingyin Liu:** Writing - reviewing & editing. **Tahmina Ajmal**: Project administration. **Abdel Aitouche**: Project administration, Funding acquisition. **Raouf Mobasheri**: Project administration. **Oyuna Rybdylova:** Writing - reviewing & editing. **Yiqiang Pei**: Methodology, Project administration, Funding acquisition. **Zhijun Peng:** Methodology, Writing - reviewing & editing.

Declaration of Competing Interest

The authors declare that they have no known competing financial interests or personal relationships that could have appeared to influence the work reported in this paper.

Acknowledgement

This work is financially supported by the National Engineering Laboratory for Mobile Source Emission Control Technology (No. NELMS2017C01), and the European Regional Development Fund (ERDF) via Interreg North-West Europe (Project No. NWE553).

Reference

[1] Awad, O.I., Ma, X., Kamil, M., Ali, O.M., Zhang, Z., Shuai, S., 2020. Particulate emissions from gasoline direct injection engines: A review of how current emission regulations are being met by automobile manufacturers. Sci. Total Environ. 718, 137302.

[2] Lyu, Y., Siddique, A.R.M., Majid, S.H., Biglarbegian, M., Gadsden, S.A., Mahmud, S., 2019. Electric vehicle battery thermal management system with thermoelectric cooling. Energy Rep. 5, 822-827.

[3] Song, Z., Pan, Y., Chen, H., Zhang, T., 2021. Effects of temperature on the performance of fuel cell hybrid electric vehicles: A review. Appl. Energy 302, 117572.

[4] Usai, L., Hung, C.R., Vásquez, F., Windsheimer, M., Burheim, O.S., Strømman, A.H., 2021. Life cycle assessment of fuel cell systems for light duty vehicles, current state-of-the-art and future impacts. J. Cleaner Prod. 280, 125086.

[5] Li, X., Peng, Z., Pei, Y., Ajmal, T., Rana, K.J., Aitouche, A., Mobasheri, R., 2022. Oxy‐fuel combustion for carbon capture and storage in internal combustion engines–A review. Int. J. Energy Res. 46(2), 505-522.

[6] Guo, J., Jiang, Y., Yu, Y., Liu, W., 2020. A novel energy consumption prediction model with combination of road information and driving style of BEVs. Sustainable Energy Technologies and Assessments, 42, 100826.

[7] Li, L., Guo, S., Cai, H., Wang, J., Zhang, J., Ni, Y., 2020. Can China's BEV market sustain without government subsidies?: An explanation using cues utilization theory. J. Cleaner Prod. 272, 122589.

[8] Qian, Y., Li, Z., Yu, L., Wang, X., Lu, X., 2019. Review of the state-of-the-art of particulate matter emissions from modern gasoline fueled engines. Appl. Energy 238, 1269-1298.

[9] Ge, J.C., Wu, G., Choi, N.J., 2022. Comparative study of pilot–main injection timings and diesel/ethanol binary blends on combustion, emission and microstructure of particles emitted from diesel engines. Fuel, 313, 122658.

[10] Chen, Z., Zhang, Y., Wei, X., Zhang, Q., Wu, Z. and Liu, J., 2017. Thermodynamic process and performance of high n-butanol/gasoline blends fired in a GDI production engine running wide-open throttle (WOT). Energy Convers. Manage. 152, 57-64.

[11] Han, D., Fan, Y., Sun, Z., Nour, M., Li, X., 2020. Combustion and emissions of isomeric butanol/gasoline surrogates blends on an optical GDI engine. Fuel 272, 117690.

[12] Huang, Y., Surawski, N.C., Zhuang, Y., Zhou, J.L., Hong, G., 2021. Dual injection: An effective and efficient technology to use renewable fuels in spark ignition engines. Renewable Sustainable Energy Rev. 143, 110921.

[13] Ikoma, T., Abe, S., Sonoda, Y., Suzuki, H., Suzuki, Y., Basaki, M., 2006. Development of V-6 3.5-liter engine adopting new direct injection system (No. 2006-01-1259). SAE Technical Paper.

[14] Daniel, R., Xu, H., Wang, C., Richardson, D., Shuai, S., 2013. Gaseous and particulate matter emissions of biofuel blends in dual-injection compared to direct-injection and port injection. Appl. Energy 105, pp.252-261.

[15] Kim, N., Cho, S., Min, K., 2015. A study on the combustion and emission characteristics of an SI engine under full load conditions with ethanol port injection and gasoline direct injection. Fuel 158, 725-732.

[16] Liu, H., Wang, Z., Long, Y., Xiang, S., Wang, J., Fatouraie, M., 2015. Comparative study on alcohol–gasoline and gasoline–alcohol Dual-Fuel Spark Ignition (DFSI) combustion for engine particle number (PN) reduction. Fuel 159, 250-258.

[17] Liu, H., Wang, Z., Long, Y., Xiang, S., Wang, J., Wagnon, S.W., 2015. Methanol-gasoline Dual-fuel Spark Ignition (DFSI) combustion with dual-injection for engine particle number (PN) reduction and fuel economy improvement. Energy 89, 1010-1017.

[18] Catapano, F., Di Iorio, S., Sementa, P., Vaglieco, B.M., 2017. Particle formation and emissions in an optical small displacement SI engine dual fueled with CNG DI and gasoline PFI (No. 2017-24-0092). SAE Technical Paper.

[19] Kang, R., Zhou, L., Hua, J., Feng, D., Wei, H., Chen, R., 2019. Experimental investigation on combustion characteristics in dual-fuel dual-injection engine. Energy Convers. Manage. 181, 15-25.

[20] Zhao, Z., Yu, X., Huang, Y., Shi, W., Guo, Z., Li, Z., Du, Y., Jin, Z., Li, D., Wang, T., Li, Y., 2022. Experimental study on combustion and emission of an SI engine with ethanol/gasoline combined injection and EGR. J. Cleaner Prod. 331, 129903.

[21] Li, D., Yu, X., Du, Y., Xu, M., Li, Y., Shang, Z., Zhao, Z., 2022. Study on combustion and emissions of a hydrous ethanol/gasoline dual fuel engine with combined injection. Fuel 309, 122004.

[22] Zhuang, Y., Hong, G., 2014. Effects of direct injection timing of ethanol fuel on engine knock and lean burn in a port injection gasoline engine. Fuel 135, 27-37.

[23] Zhuang, Y., Ma, Y., Qian, Y., Teng, Q., Wang, C., 2020. Effects of ethanol injection strategies on mixture formation and combustion process in an ethanol direct injection (EDI) plus gasoline port injection (GPI) spark-ignition engine. Fuel 268, 117346.

[24] Li, X., Pei, Y., Ajmal, T., Rana, K.J., Aitouche, A., Mobasheri, R., Peng, Z., 2021. Numerical investigation on implementing Oxy-Fuel Combustion (OFC) in an ethanol-gasoline Dual-Fuel Spark Ignition (DFSI) engine. Fuel, 302, 121162.

[25] Holman, J.P., 1966. Experimental methods for engineers. New York, NY: McGraw-Hill.

[26] Hung, D.L., Harrington, D.L., Gandhi, A.H., Markle, L.E., Parrish, S.E., Shakal, J.S., Sayar, H., Cummings, S.D., Kramer, J.L., 2009. Gasoline fuel injector spray measurement and characterization–a new SAE J2715 recommended practice. SAE International Journal of Fuels and Lubricants 1(1), 534-548.

[27] Symonds, J.P.R., 2010. Calibration of fast response differential mobility spectrometers. National Physical Lab., Metrology of Airborne Nanoparticles, Standardisation and Applications, London.

[28] Chen, L., Liang, Z., Zhang, X., Shuai, S., 2017. Characterizing particulate matter emissions from GDI and PFI vehicles under transient and cold start conditions. Fuel 189, 131-140.

[29] Wang, H., Frenklach, M., 1997. A detailed kinetic modeling study of aromatics formation in laminar premixed acetylene and ethylene flames. Combust. Flame 110(1-2), 173-221.

[30] Sun, W., Hamadi, A., Abid, S., Chaumeix, N., Comandini, A., 2020. An experimental and kinetic modeling study of phenylacetylene decomposition and the reactions with acetylene/ethylene under shock tube pyrolysis conditions. Combust. Flame 220, 257-271.